

Andreas Mutzke, Ralf Schneider

**SDTrimSP-2D: Simulation des Teilchenbeschusses auf
zweidimensionale Targets
Version 1.0**

**SDTrimSP-2D: Simulation of Particles Bombarding on a Two
Dimensional Target
Version 1.0**

SDTrimSP-2D: Simulation of Particles Bombarding on a Two Dimensional Target

Version 1.0

A. Mutzke, R.Schneider

Contents

1. Introduction	2
2. basic physic	3
3. Geometry	4
4. Beam	5
4.1. polar and azimuthal angle of incidence	5
4.2. Incident energy of projectiles	6
5. Target	7
5.1. Change of cell volume	7
5.2. Dynamical relaxation of the target	10
5.3. Change of density and target fraction in a cell	14
5.4. Detect corresponding cell of particle location in the target	15
5.5. Cases of deleted cells in the target	16
5.6. Creation of a hole in the target	18
5.7. Vertical relaxation in target	22
5.8. Influence of the resolution	25
6. Comparison of SDtrimSP and SDTrimSP-2D	27
7. Two-Dimensional examples with SDTrimSP-2D	29
7.1. 1000 eV Xe on Si	29
7.2. 6 keV C on W	34
A. Unit of physical terms	37

1. Introduction

The new program is an extension of the one dimensional codes TRIMM, TRIDYN and SDTrimSP (Static and Dynamic Trim for Sequential and Parallel computer) described in [2], [3], [4] and [5]. These programs simulate the interaction of energetic particle with solid in the binary collision approximation.

The particles (projectiles) impinging on the target, can be neutral atoms or ions. The ions experience the sheath in front of the wall and arrive at the surface as neutral atoms with increased energy due to the acceleration in the sheath. If a projectile penetrates a solid target it will be scattered due to elastic collisions with target atoms, which lead to a change of energy and direction. In addition, the projectiles can suffer inelastic energy losses due to collisions with electrons. When the projectiles have lost all their energy, they are deposited in the target. Other possibilities are that the projectiles are backscattered after some collisions or are transmitted.

The energy lost by a projectile in an elastic collision is transferred to the target atom and a recoil is created. This can collide again with other target atoms. If its energy is large enough the recoil can also leave the target (backward or transmission sputtering). The trajectories of particles take place in three dimensions. Up to now, the target was considered to be only one dimensional. It consisted of layers, which have different thickness and varying composition.

In this new program version the target is treated as two dimensional. This allows studies of new effects like morphological changes of the surface and the influence of roughness on scattering and sputtering.

2. basic physic

The computer simulation of atomic collision is based in this model on the binary collision approximation.

The coordinate system X_1, Y_1, Z_1 is adjusted so that the x-axis is the flight direction of the projectile before a collision. The position of projectiles is marked with P (P_0, P_1, P_2) and recoils with T , (T_0, T_1).

Fig. 1 shows this basic coordinate system used already in all previous programs including SDTrimSP.

The mean-free path l_m , see [1] and [4], between two collisions is calculated using the local atomic density ϱ :

$$l_m = \varrho^{-1/3}. \quad (2.1)$$

The actual impact parameter is:

$$P_{\text{impact}} = \sqrt{R_{\text{random}}} \cdot \frac{l_m}{\sqrt{2 \cdot \pi}} \quad R_{\text{random}}: \text{random number} \quad (2.2)$$

The scattering angle ϑ_1 and the recoil angle ϑ_2 can be computed from the center-of-mass scattering angle $\bar{\vartheta}$.

More detailed descriptions of all the physics can be found in [2].

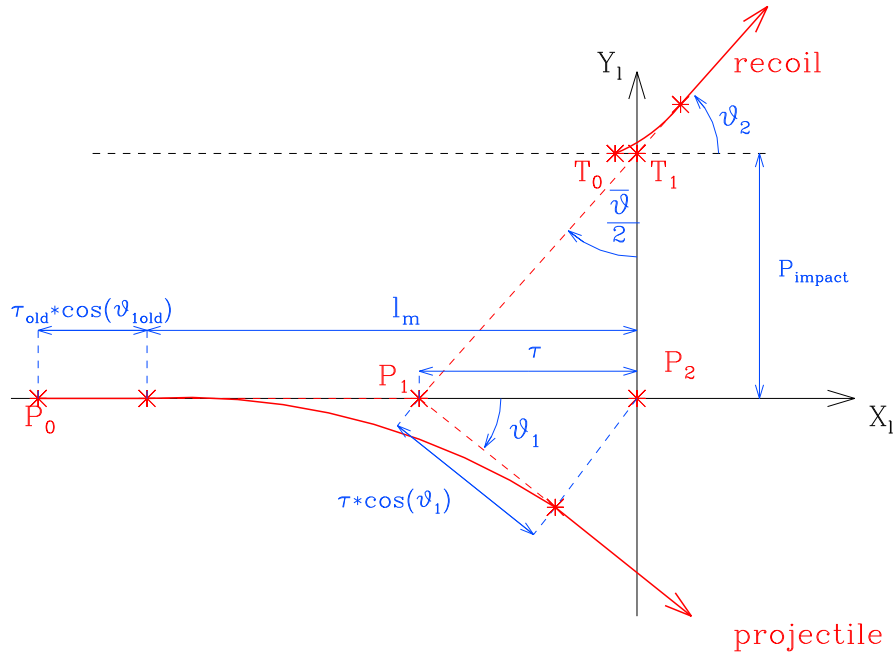


Figure 1: Geometry of a binary collision

3. Geometry

A right-handed coordinate system (X_{3D}, Y_{3D}, Z_{3D}) is used in the new code. The polar and azimuthal angle are the same as in SDTrimSP.

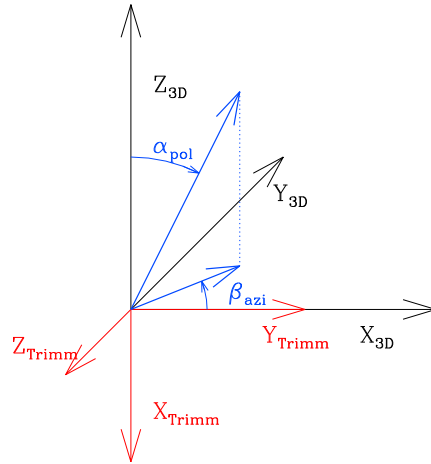


Figure 2: Definition of the coordinates, the polar angle and azimuthal angle

In the new code target cells are introduced. Each cell has 6 surfaces and 6 directions, see Fig. 3.

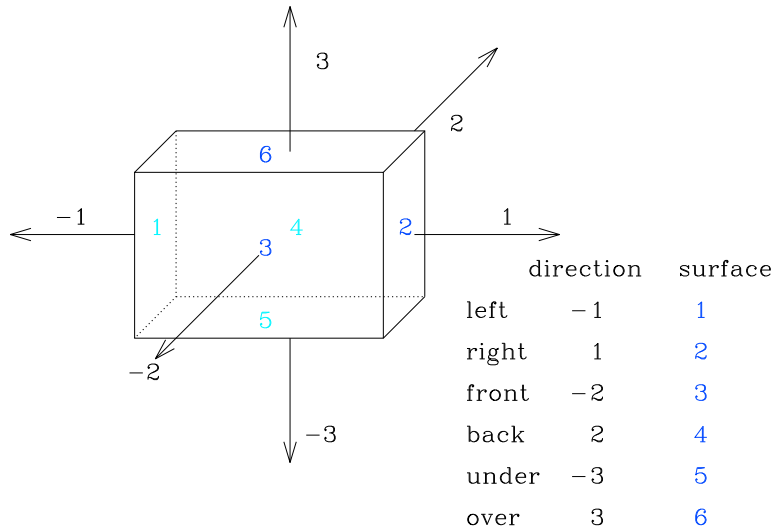


Figure 3: Index of the directions and the surfaces of one target cell

4. Beam

4.1. polar and azimuthal angle of incidence

The polar angle is α_{pol} . The range is $[0 \dots \pi/2]$

The azimuthal angle is φ_{azi} . The range is $[0 \dots 2\pi]$

Cases of angular distributions of the impinging particles:

0 : polar angle is constant ($\alpha_{pol} = \alpha_0$, $\varphi_{azi} = 0$)

1 : random distribution of angles ($\alpha_{pol} = 0 \dots \pi/2$, $\varphi_{azi} = 0 \dots 2\pi$)

2 : cosine distribution of angles ($\alpha_{pol} = 0 \dots \pi/2$,max: by 45 , $\varphi_{azi} = 0 \dots 2\pi$)

3 : cosine distribution of angles ($\alpha_{pol} = 0 \dots \pi/2$,max: by 0 , $\varphi_{azi} = 0 \dots 2\pi$)

4 : given distribution of polar angles file:fa.inp ($\varphi_{azi} = 0$)

5 : series of of calculations ($\alpha_{pol} = (i - 1) \cdot \alpha_0$, $\varphi_{azi} = 0$)

6 : polar angle has a Gaussian distribution ($\varphi_{azi} = 0$)

$$\text{mean: } \alpha_0 = \frac{1}{n} \cdot \sum \alpha \quad (4.3)$$

$$\text{standard diviation: } \Delta\alpha = \frac{1}{n-1} \cdot \sum (\alpha - \alpha_0) \quad (4.4)$$

$$\text{frequency function: } p = \frac{1}{\sqrt{2 \cdot \Pi \Delta\alpha^2}} \cdot e^{-\frac{(\alpha - \alpha_0)^2}{2\Delta\alpha^2}} \quad (4.5)$$

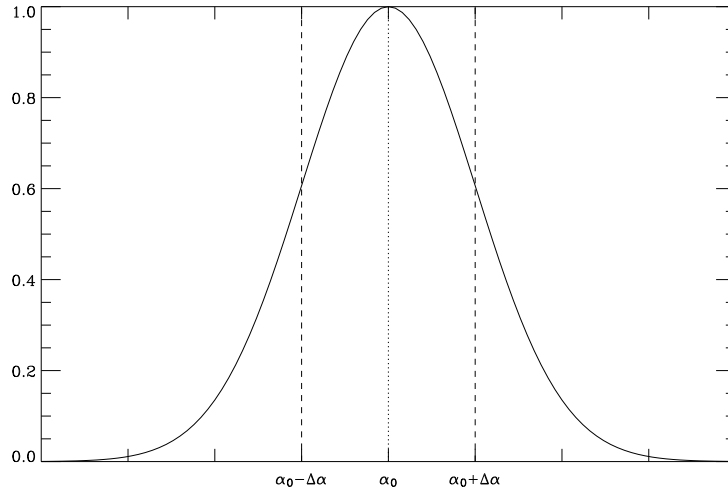


Figure 4: Gaussian frequency distribution ($p \cdot \sqrt{2 \cdot \Pi \Delta\alpha^2}$) of polar angles (case 6)

4.2. Incident energy of projectiles

The beam energy is e_{part} . The range is [1eV...100MeV]

Case of energy distributions of the impinging particles:

- 0 : constant energies (in eV) for projectiles
- 1 : input of a given energy distribution (file: fe.inp)
- 2 : temperature (in eV) of a Maxwellian velocity distribution
- 3 : temperature (in eV) of a Maxwellian energy distribution
- 5 : series of calculations ($e_{part} = i \cdot e_0$)
- 6 : Gaussian distribution

$$\text{mean: } e_0 = \frac{1}{n} \cdot \sum e \quad (4.6)$$

$$\text{standard deviation: } \Delta e = \frac{1}{n-1} \cdot \sum (e - e_0) \quad (4.7)$$

$$\text{frequency function: } p = \frac{1}{\sqrt{2 \cdot \Pi \Delta e^2}} \cdot e^{-\frac{(e-e_0)^2}{2\Delta e^2}} \quad (4.8)$$

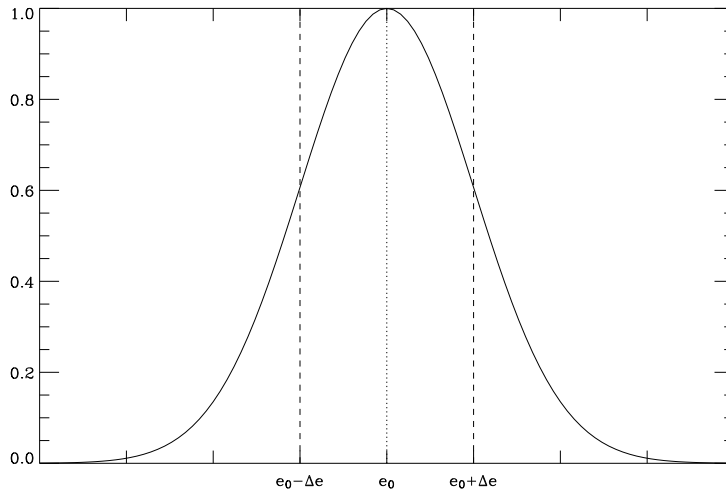


Figure 5: Gaussian distribution ($p \cdot \sqrt{2 \cdot \Pi \Delta e^2}$) of energy (case 6)

5. Target

5.1. Change of cell volume

The numbers of deposited, backscattered or transmitted particles $N_1(j)$ are calculated after the bombardment of the target with NR pseudo-particles (in program: `nr_pproj`). Due to the deposition or loss of particles the composition of target is changed. The probability that one incident particle change the number of atoms in one cell is N_2 :

$$N_2(j) = \frac{N_1(j)}{NR} \quad [-] \quad j \dots \text{species of atoms (in program: } j = 1 \dots ncp) \quad (5.9)$$

The fluence step is:

$$\Delta flc = \frac{\text{fluence}}{\text{number histories}} \quad \left(\text{ in program: } fluc_step = \frac{flc}{maxhist} \right) \quad (5.10)$$

SDTrimSP

In the program SDTrimSP the absolute number of atoms in one layer is $N_3(j)$ (normalized to $\Delta x \cdot \Delta y$). The thickness of this layer is Δz , the atomic fraction is qu and the density is ϱ . The new thickness of the layer z_{new} and the new volume V_{new} of one layer is calculated from:

$$N_3^{1D}(j) = N_2(j) \cdot \Delta flc + qu_{old}(j) * \varrho_{old} * \Delta z \quad (5.11)$$

$$z_{new} = \sum \frac{N_3^{1D}(j)}{\varrho_0(j)} \quad (5.12)$$

$$V_{new} = z_{new} \cdot \Delta x \cdot \Delta y = \sum \frac{N_3^{1D}(j)}{\varrho_0(j)} \cdot \Delta x \cdot \Delta y. \quad (5.13)$$

This is changed for an area ($\Delta x \cdot \Delta y$):

$$N_3^{3D}(j) = N_2(j) \cdot \Delta flc \cdot \Delta x \cdot \Delta y + qu_{old}(j) * \varrho_{old} * \Delta V \quad (5.14)$$

$$V_{new} = \sum \frac{N_3^{3D}(j)}{\varrho_0(j)} \quad (5.15)$$

SDTrimSP-2D

In the program with a 2-D-target the absolute number of the atoms in one cell is the sum of new deposited atoms and old atoms after one fluence step:

$$N_3(j) = N_2(j) \cdot \Delta f_{lc} \cdot A_{flc} + qu_{old}(j) * \varrho_{old} * V \quad (5.16)$$

$$(5.17)$$

The new Volume is:

$$V_{new} = \sum \frac{N_3(j)}{\varrho_0(j)} \quad (5.18)$$

The target in SDTrimSP-2D can be one or two dimensional (or three dimensional in the future).

In 1-D, the Δx and Δy must be greater than the maximum of x or y values of a typical particle cascade. This is the same geometry as in the code SDTrimSP.

In this case, the real beam surface A_{flc} can be calculated as:

$$A_{flc} = \Delta x_{cell} \cdot \Delta y_{cell} \quad (1-D) \quad (5.19)$$

In 2-D, Δy must be greater than the maximum of y values of the particle cascade. Δx is the beam width.

In this case, the real beam surface A_{flc} can be calculated as:

$$A_{flc} = \Delta x_{beam} \cdot \Delta y_{cell} \quad (2-D) \quad (\text{in program: } A_{flc} \dots \text{beam_geo_fac}) \quad (5.20)$$

In 3-D, A_{flc} dependent on beam geometry only.

$$A_{flc} = \Delta x_{beam} \cdot \Delta y_{beam} \quad (3-D) \quad (5.21)$$

The atomic composition of the target has ncp species with atomic fractions qu

$$\sum_{j=1}^{ncp} qu(j) = 1 \quad (5.22)$$

In some cases, it is necessary to define a maximum allowed atomic fraction. This maximum atomic fraction qu_a^{max} can be defined in order to simulate local saturation phenomena, see [3].

For a given maximum atomic fraction of one species (a) the number of particles can be calculated :

$$N_3(a)^{max} = \frac{qu_a^{max}}{1 - qu_a^{max}} \cdot \left(\sum_{j=1}^{ncp} N_3(j) - N_3(a) \right) \quad (5.23)$$

$$N_4(a) = \max(N_3(a)^{max}, N_3(a)) \quad (5.24)$$

If two maxima qu_a^{max} and qu_b^{max} are given for species a and b then the number of particles are :

$$Q_a = \frac{qu_a^{max}}{1 - qu_a^{max}} \quad (5.25)$$

$$Q_b = \frac{qu_b^{max}}{1 - qu_b^{max}} \quad (5.26)$$

$$N_4(a) = \frac{Q_a \cdot Q_b + Q_a}{1 - Q_a \cdot Q_b} \cdot \left(\sum_{j=1}^{ncp} N_3(j) - N_3(a) - N_3(b) \right) \quad (5.27)$$

$$N_4(b) = Q_b \cdot \left(\sum_{j=1}^{ncp} N_3(j) - N_3(a) - N_3(b) + N_4(a) \right) \quad (5.28)$$

The volume change of the cell is:

$$\Delta V = \sum_{j=1}^{ncp} \frac{N_4(j)}{\varrho_0(j)} - V. \quad (5.29)$$

$N_4(j)$ is the number of particles in the cell of species j in the Volume $V + \Delta V$.

5.2. Dynamical relaxation of the target

The thermal expansion of solids [1] can be described as:

$$\begin{aligned}\Delta l &= l \cdot \alpha \cdot \Delta T \\ \Delta V &= V \cdot \beta \cdot \Delta T\end{aligned}\tag{5.30}$$

The dynamical relaxation of the target is treated as a volume expansion similar to the thermal expansion.

$$\Delta l = l \cdot k'\tag{5.31}$$

The assumption is used that the cell is a brick with edge lengths a,b,c and the volume increase of volume is the sum of the expansions in all directions d . The expansion of each side is considered. The increase of volume ΔV is given as

$$\begin{aligned}\Delta l_d &= l_d \cdot \frac{k'}{2} \quad (d = 1\dots 6) \\ \Delta l_d &= l_d \cdot k\end{aligned}\tag{5.32}$$

$$\begin{aligned}\Delta l_a &= k' \cdot a = 2 \cdot k \cdot a \\ \Delta l_b &= k' \cdot b = 2 \cdot k \cdot b \\ \Delta l_c &= k' \cdot c = 2 \cdot k \cdot c\end{aligned}\tag{5.33}$$

$$\Delta V = \Delta l_a \cdot b \cdot c + \Delta l_b \cdot a \cdot c + \Delta l_c \cdot a \cdot b\tag{5.34}$$

$$\Delta V = 2 \cdot k \cdot a \cdot b \cdot c + 2 \cdot k \cdot b \cdot a \cdot c + 2 \cdot k \cdot c \cdot a \cdot b\tag{5.35}$$

$$\Delta V = 6 \cdot k \cdot a \cdot b \cdot c\tag{5.36}$$

$$\Delta V = 6 \cdot k \cdot V\tag{5.37}$$

$$\tag{5.38}$$

The change of Volume is assumed to be the same in all directions.

$$k = \frac{\Delta V}{6 \cdot V}\tag{5.39}$$

$$k = \frac{\Delta V}{fgrd \cdot V}\tag{5.40}$$

$$k_c = \frac{\Delta V_c}{fgrd_c \cdot V_c}\tag{5.41}$$

with: $fgrd$ are asymmetry factors to be chosen and c is the index of the cell.

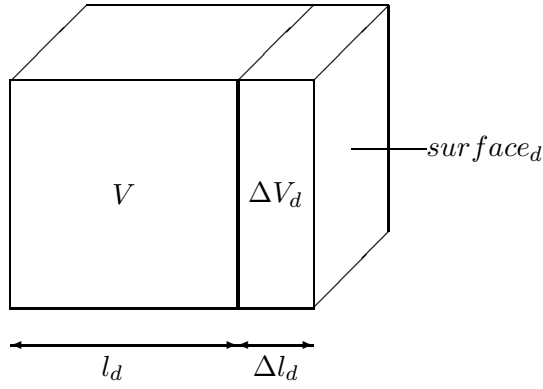


Figure 6: Geometry of cell

The area (or a part) of a side is the surface (*surf*). The volume expansion in each direction (d) is:

$$\Delta V_d = surf_d \cdot \Delta l_d \quad (5.42)$$

d is the index of flux at each surface or direction of cell. The range of d is 1 to 6. The index of cell is c.

Replace Δl_d with equation 5.32 and 5.41:

$$\Delta V_d = surf_d \cdot k_c \cdot l_d \quad (5.43)$$

$$\Delta V_d = surf_d \cdot \frac{\Delta V_c}{fgd_c \cdot V_c} \cdot l_d \quad (5.44)$$

$$\Delta V_d = \Delta V_c \cdot \frac{surf_d \cdot l_d}{fgd_c \cdot V_c} \quad (5.45)$$

$$\sum \Delta V_d = \Delta V_c \quad \text{without wight factor} \quad (5.46)$$

The volume-flux ΔV_d through a surface can be modified using a weight factor *wig* (default: $wig = 1.0$).

It is a possibility to control the anisotropy of the particle fluxes in the target with the help of this factor *wig*.

$$\Delta V_d = \Delta V_c \cdot \left(\frac{surf_d \cdot l_d}{fgd_c \cdot V_c} \cdot wig_d \right) \quad (5.47)$$

$$\Delta V_d = \Delta V_c \cdot fac \quad (\text{in program: } cel_flux(d)val = cel_dvol(c) \cdot cel_fak(d))$$

The volume fluxes are calculated in the subroutine flux_vol.

$$\sum \Delta V_d \leq \Delta V_c \quad \text{with wight} \quad (5.48)$$

5. Target

To calculate the volume change (volume flux) between the cells the diffusion equation is used.

$$\frac{\partial V}{\partial \tau} = \frac{\partial D \cdot \frac{\partial V}{\partial x}}{\partial x} + \frac{\partial D \cdot \frac{\partial V}{\partial y}}{\partial y} + \frac{\partial D \cdot \frac{\partial V}{\partial z}}{\partial z} \quad (5.49)$$

For a two dimensional target, the equation has only two terms:

$$\frac{\partial V}{\partial \tau} = \frac{\partial D \cdot \frac{\partial V}{\partial x}}{\partial x} + \frac{\partial D \cdot \frac{\partial V}{\partial z}}{\partial z} \quad (5.50)$$

The finite-difference form is upstream in pseudo time and centered in space:

$$\frac{\Delta V}{\Delta \tau} = \frac{(D \cdot \Delta V_{right} - D \cdot \Delta V_{left})}{\Delta x^2} + \frac{(D \cdot \Delta V_{top} - D \cdot \Delta V_{bottom})}{\Delta z^2} \quad (5.51)$$

with

$$\begin{aligned} \frac{\Delta \tau \cdot D \cdot \Delta V_{left}}{\Delta x^2} &= \frac{sur_{left} \cdot l_x}{f_{grd_c} \cdot V_c} \cdot wig_{left} \cdot \Delta V_c = f_{c,l} \cdot \Delta V_c \\ \frac{\Delta \tau \cdot D \cdot \Delta V_{right}}{\Delta x^2} &= \frac{sur_{right} \cdot l_x}{f_{grd_c} \cdot V_c} \cdot wig_{right} \cdot \Delta V_c = f_{c,r} \cdot \Delta V_c \\ \frac{\Delta \tau \cdot D \cdot \Delta V_{bottom}}{\Delta z^2} &= \frac{sur_{bottom} \cdot l_z}{f_{grd_c} \cdot V_c} \cdot wig_{bottom} \cdot \Delta V_c = f_{c,b} \cdot \Delta V_c \\ \frac{\Delta \tau \cdot D \cdot \Delta V_{top}}{\Delta z^2} &= \frac{sur_{top} \cdot l_z}{f_{grd_c} \cdot V_c} \cdot wig_{top} \cdot \Delta V_c = f_{c,t} \cdot \Delta V_c \end{aligned}$$

$$\begin{aligned} \Delta V_{\tau,i,k} - \Delta V_{\tau-1,i,k} &= \\ & [(f_{i+1,l} \cdot \Delta V_{i+1} - f_{i,r} \cdot \Delta V_i) - (f_{i,l} \cdot \Delta V_i - f_{i-1,r} \cdot \Delta V_{i-1})]_{\tau-1,k} \\ & + [(f_{k+1,b} \cdot \Delta V_{k+1} - f_{k,t} \cdot \Delta V_k) - (f_{k,b} \cdot \Delta V_k - f_{k-1,t} \cdot \Delta V_{k-1})]_{\tau-1,i} \end{aligned} \quad (5.52)$$

In the case that only expansion in positive z-direction is assumed (like in the 1-D-Model SDTrimSP):

$$\frac{\partial V}{\partial \tau} = D \cdot \frac{\partial^2 V}{\partial z^2} \quad (5.53)$$

with

$$\begin{aligned} f_{c,l} &= 0 \\ f_{c,r} &= 0 \\ f_{c,b} &= 0 \\ f_{c,t} &= 1 \end{aligned}$$

The finite-difference form is :

$$\Delta V_{\tau,k} = (-\Delta V_k + \Delta V_{k-1}) \quad (5.54)$$

The initial condition for equation 5.52 is:

$$\Delta V(\tau = 0) = \Delta V_c \quad (5.55)$$

$$(5.56)$$

The boundary conditions are:

top : open boundary condition

bottom : open boundary condition

left : $(\Delta V_{i-1} - \Delta V_i)|_{\tau-1,j,k} = 0, (i = 1)$

right : $(\Delta V_i - \Delta V_{i+1})|_{\tau-1,j,k} = 0, (i = i_{max})$

In the case of a periodical target the boundary conditions are:

left : $(\Delta V_{i-1} = \Delta V_{max})$

right : $(\Delta V_{max+1} = \Delta V_1)$

The steady-state solution of the equations 5.52 and 5.54 are the volume fluxes (celflux):

$$\Delta V(\tau \rightarrow \infty) = 0 \quad (5.57)$$

$$celflux_{right} = \sum_{\tau=0}^{\tau=\infty} (\Delta V_{i,j,k} - \Delta V_{i+1,j,k}) \quad (5.58)$$

$$celflux_{left} = \sum_{\tau=0}^{\tau=\infty} (\Delta V_{i-1,j,k} - \Delta V_{i,j,k}) \quad (5.59)$$

$$celflux_{top} = \sum_{\tau=0}^{\tau=\infty} (\Delta V_{i,j,k} - \Delta V_{i,j,k}) \quad (5.60)$$

$$celflux_{bottom} = \sum_{\tau=0}^{\tau=\infty} (\Delta V_{i,j,k-1} - \Delta V_{i,j,k+1}) \quad (5.61)$$

The calculation of volume-flux in x and z directions is introduced in the 2-D program. Due to this volume transport a material flux to the neighbouring cells exists.

5.3. Change of density and target fraction in a cell

The number of particles in a cell coming from neighbouring cells is :

$$N_{in}(j) = \sum^m \frac{celflux(m)}{V(m) + dV(m)} * N_4(m, j) \quad j...species\ of\ atoms \quad (5.62)$$

with m is index of neighbouring cells.

This defines a volume change:

$$dV_{in} = \sum^m celflux(m) \quad (5.63)$$

The volume of a cell in the target is constant and is independent of flux, therefore the incoming flux has to balance the outflow.

$$dV_{out} = dV_{in} \quad (5.64)$$

The number of particles in the cell is:

$$N_5(j) = N_{in}(j) + \frac{(V - dV_{out})}{V + dV} * N_4(j) \quad (5.65)$$

The composition is:

$$qu(j) = N_5(j) / \sum_{k=1}^n (N_5(k)) \quad j...species\ of\ atoms \quad (5.66)$$

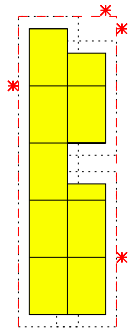
The next step is the calculation of the new density.

$$\frac{1}{\varrho} = \sum_{k=1}^n \frac{celqu(k)}{\varrho_0(k)} \quad (5.67)$$

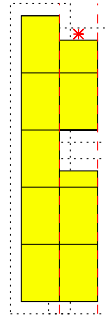
5.4. Detect corresponding cell of particle location in the target

The search algorithm of the actual cell for the particle trajectories is computed in the subroutine *xyz_in_cel*. The different cases are:

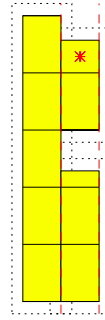
case 1.0



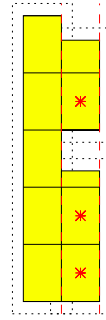
case 2.1



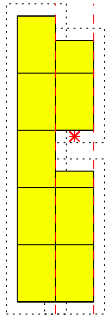
case 2.2



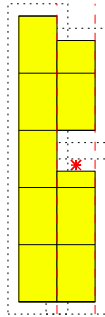
case 2.3



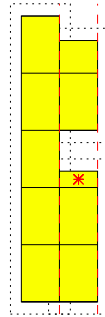
case 2.4



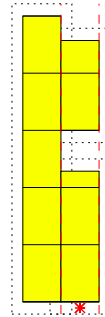
case 2.5



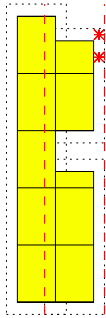
case 2.6



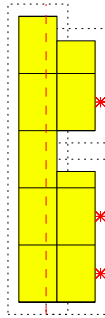
case 2.7



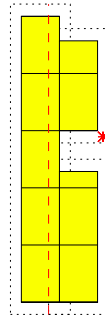
case 3.1



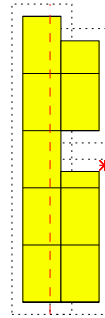
case 3.3



case 3.4



case 3.5



case 3.6

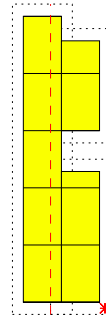


Figure 7: Cases of particle location

5.5. Cases of deleted cells in the target

After each fluence step (several cascades are computed) the composition in each cell may be changed, because particles can be implanted or damage can be created. In the subroutine *change_vol* the target geometry is corrected according to these changes.

Cells at the surface (above or below the surface) can only expand or shrink. In general, there exist 3 cases of cell changes in the program.

The volume of a cell can change without adding a new cell or deleting a cell (case 1).

A new cell is created with the status above/below, because the new cell volume is greater than a maximum (case 2).

If the reduction of the volume is greater than the volume of the cell the cell is deleted and the next cell get the status above/below and decreases (case 3).

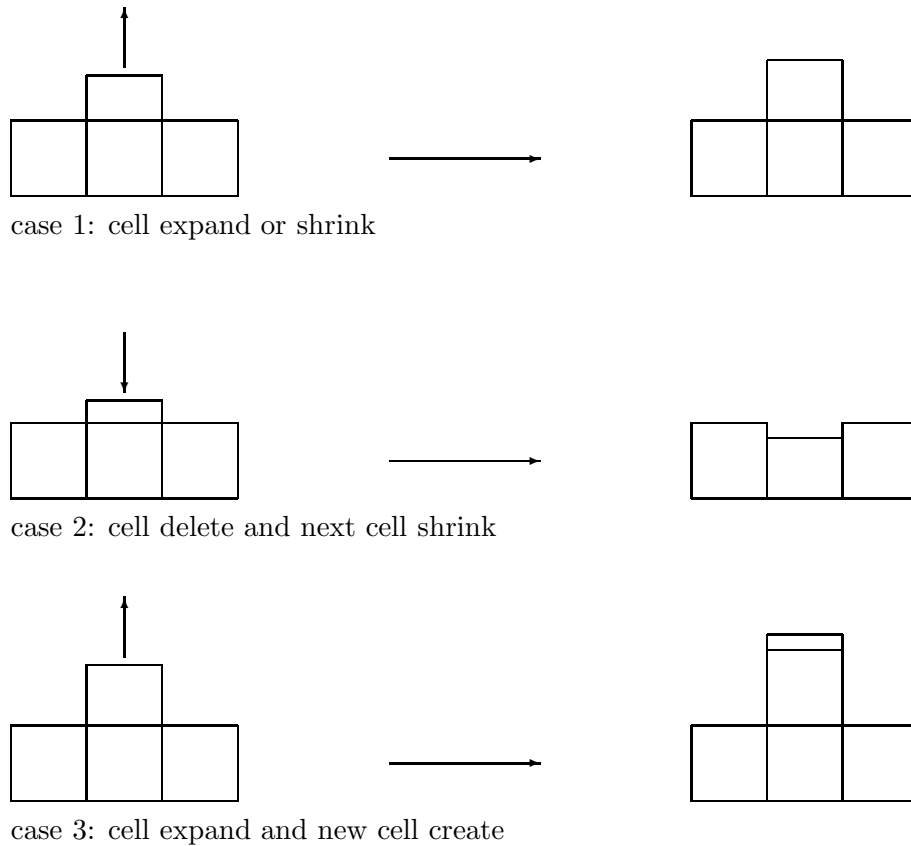


Figure 8: Possible change of above cells

According to the cell-geometry, see Fig. 9, eight cases of deleting cells exist:

- a.1: cell is above and below, next cell does not exist
- a.2: cell is above and not below, next cell exists
- a.3: cell is above and below a hole, next cell exists
- b.1: cell is above of a hole, next cell does not exist
- b.2: cell is above of a hole, next cell exists
- b.3: cell is above of a hole and below a hole, next cell exists
- c.1: cell is not above and below, next cell does not exist
- c.2: cell is not above and below of a hole, next cell exists

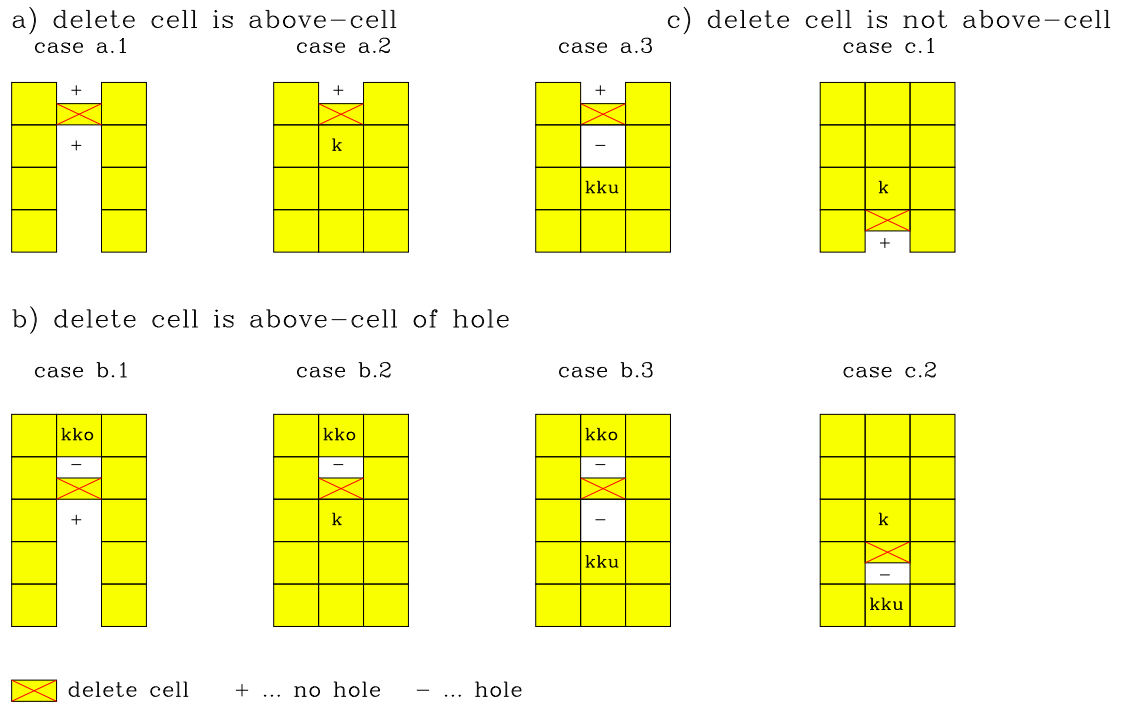


Figure 9: Cases of deleting cells in subroutine *change_vol*

5.6. Creation of a hole in the target

The expansion of material produces tension in the target. Depending on the material there exists a maximum of tension the material can withstand. If the tension or expansion is greater than this maximum then the material breaks, [6], [7], see Fig. 10. A hole is generated in the target, see Fig. 11.

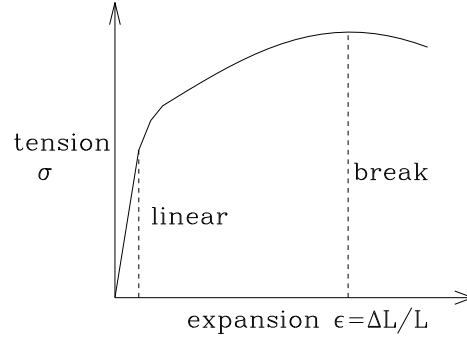


Figure 10: Tension - expansion - diagram

The condition to break a cell or to make a hole is taken as

$$\frac{\sum \Delta V_{in}}{V} > 0.5 \quad (5.68)$$

This corresponds to an expansion

$$\epsilon = \frac{\Delta L}{L} > 0.5 \quad (5.69)$$

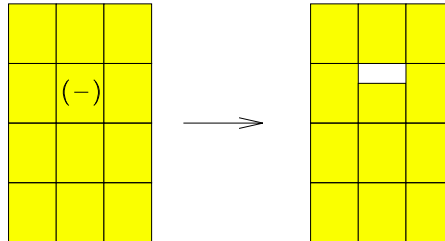


Figure 11: Breaking of a cell, a hole is generated

Holes are closed, if the volumes of cells below and above are greater than the hole.
 According to the geometry of the target there exists one case to close the hole and three cases to change it, see Fig. 12.

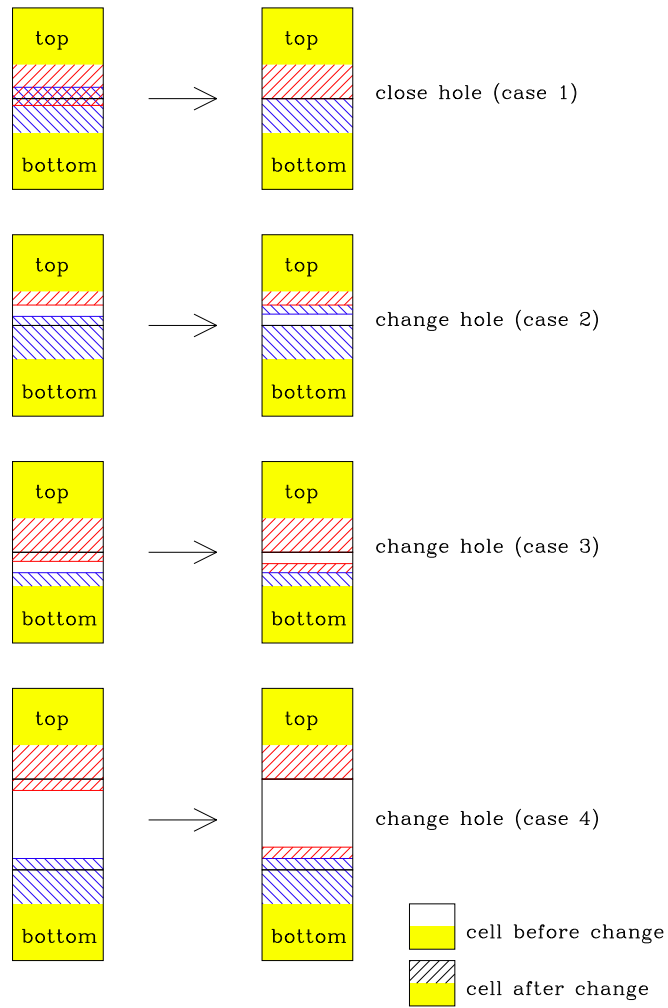


Figure 12: Cases of closing and changing a hole

5. Target

The reverse of a hole generation is the swelling of cells, see Fig. 13.

The swelling of a cell is restricted, that the cell has only a free surface in x direction.

The condition for swelling a cell is taken as

$$\frac{\sum \Delta V_{out}}{V} > 0.5 \quad (5.70)$$

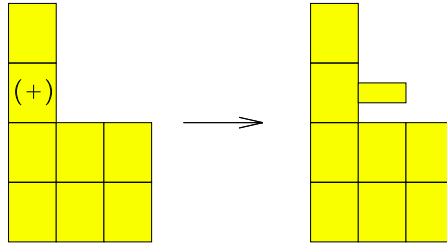


Figure 13: Swell of a cell

A simulation of the interaction of a Xe beam with a Si target for an angle of incidence of 30 degrees with and without hole algorithm is shown in Fig. 14 and Fig. 15.

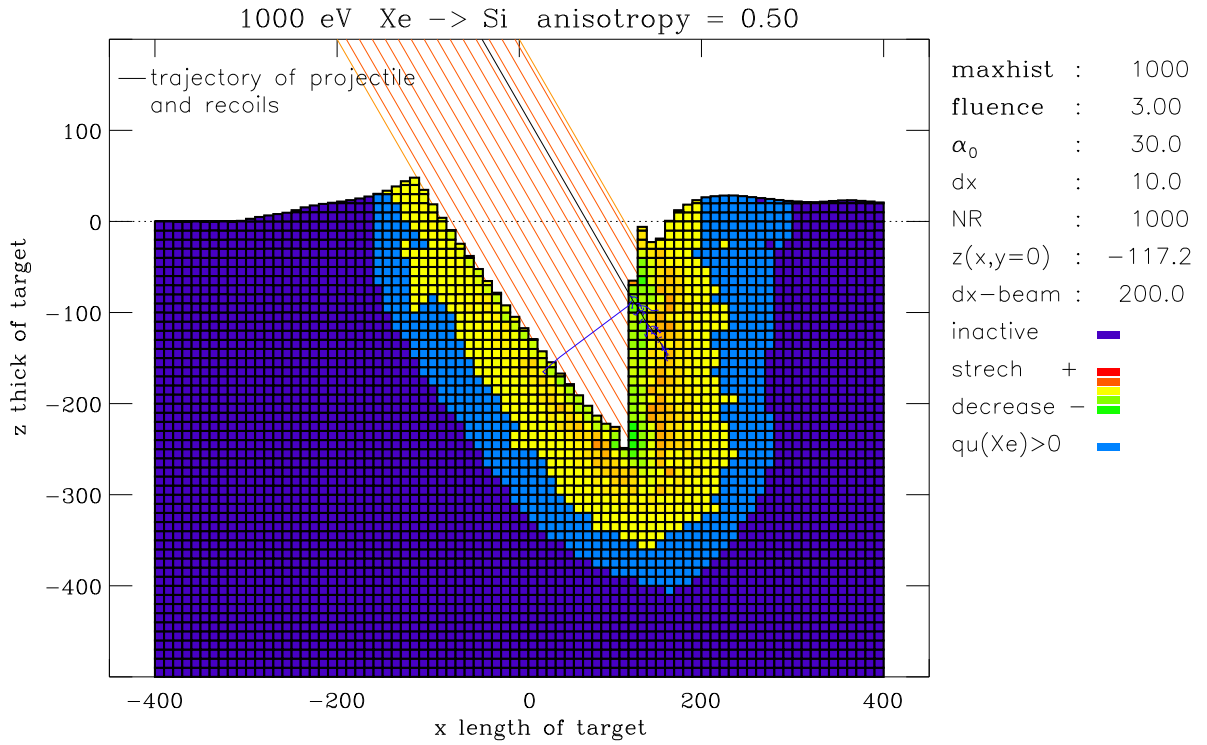


Figure 14: A target simulation without holes

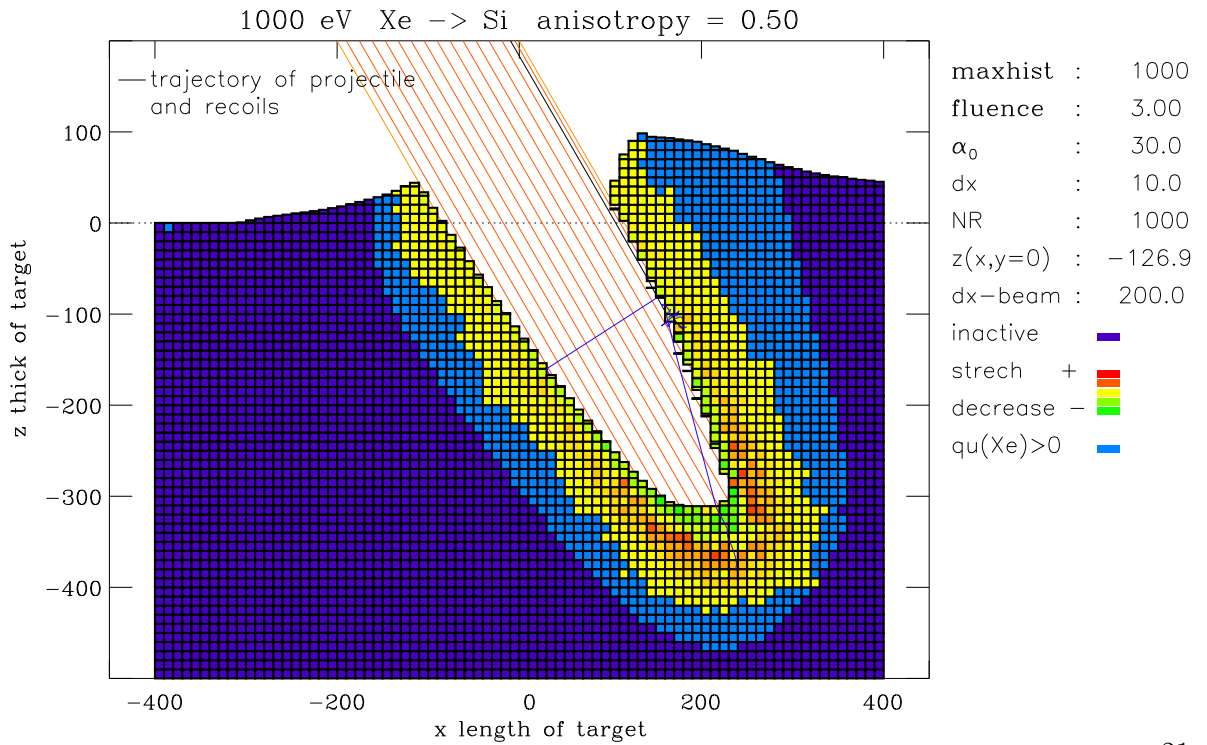


Figure 15: A target simulation with holes

5.7. Vertical relaxation in target

The dynamic relaxation of the target occurs in the 1-D model SDTrimSP only in the horizontal direction.

Fig. 16 shows a simulation without vertical relaxation, like in the 1D-program. The vertical relaxation is also necessary for numerical stability, similar to the diffusion in numerical calculations of conduction-convection problems.

In the 2-D model, it is possible to consider also relaxation in vertical direction. The value may be dependent on the material of the target.

Fig. 17 - Fig. 20 show targets with different vertical relaxations. Only the simulations with an anisotropy factor greater than 0.50 produce reasonable results.

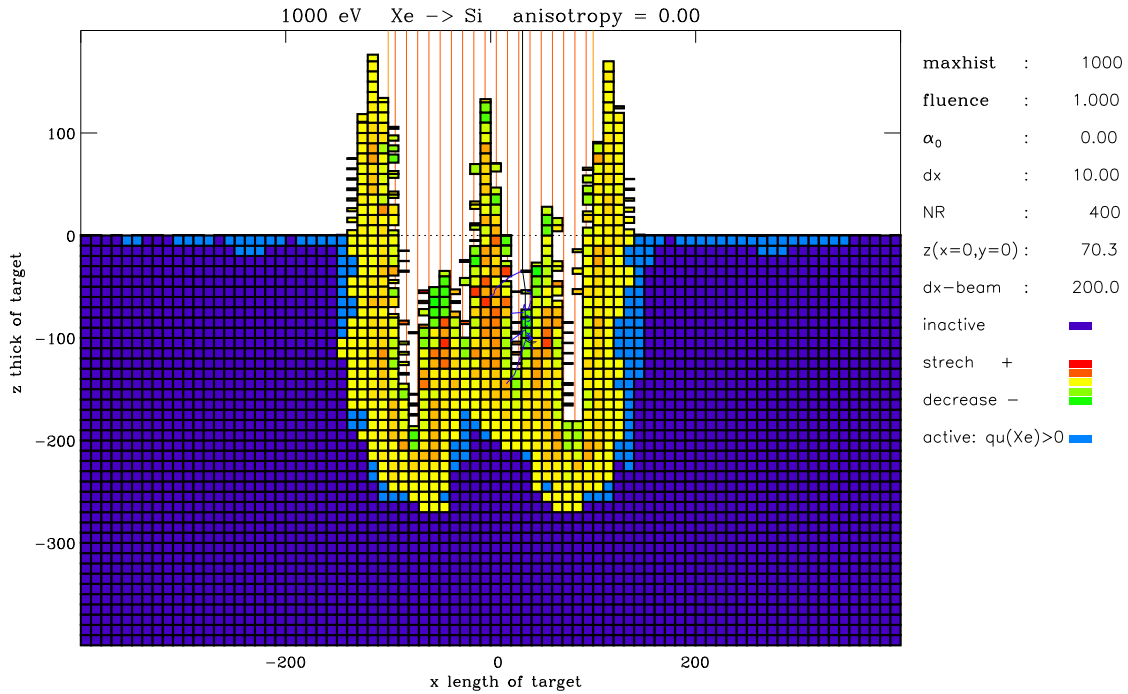
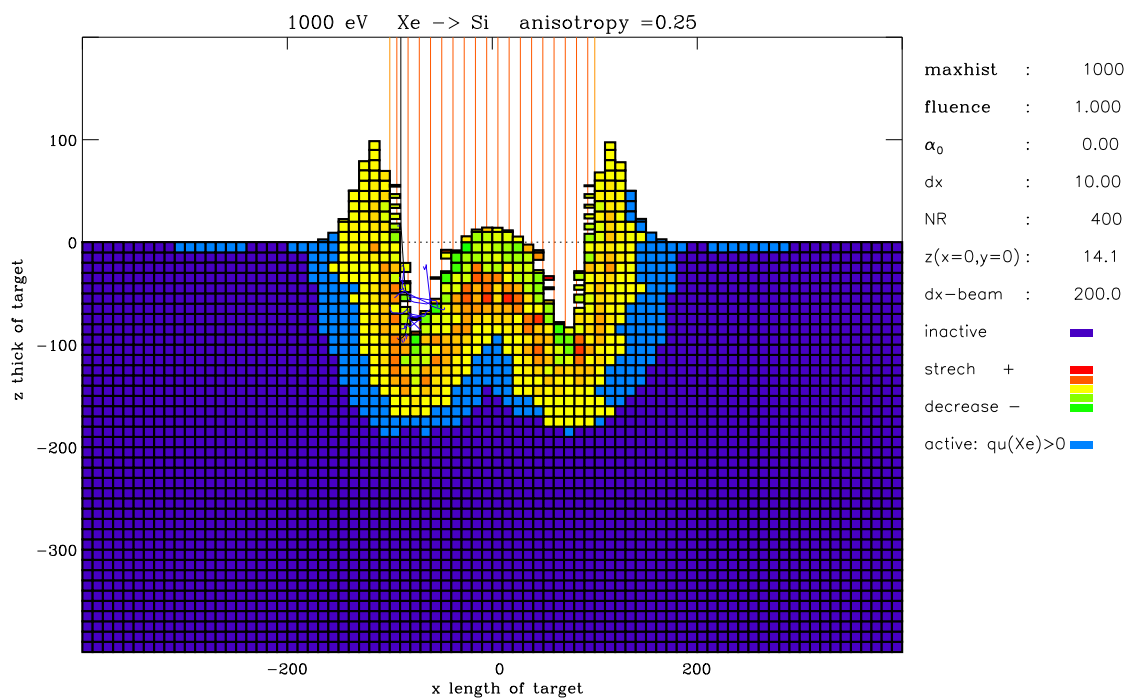
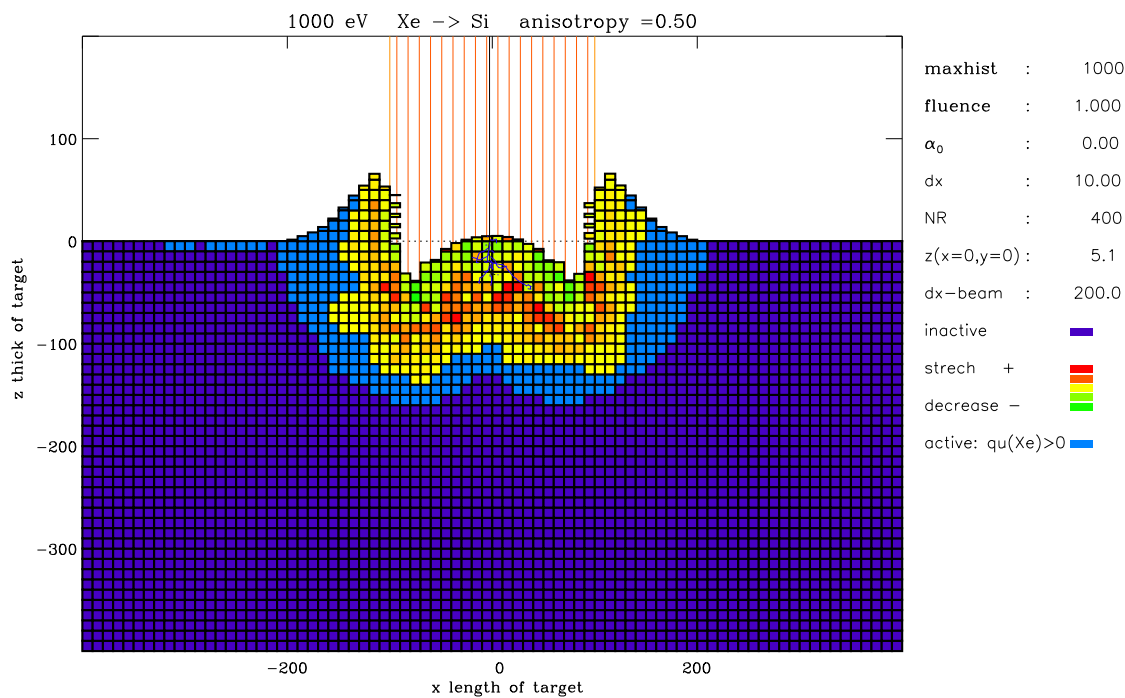


Figure 16: The target without vertical relaxation (anisotropy=0) $\Delta x_{beam} = 200 \text{ \AA}$

Figure 17: The target with small vertical relaxation (anisotropy=0.25), $\Delta x_{beam} = 200 \text{ \AA}$ Figure 18: The target with vertical relaxation (anisotropy=0.50), $\Delta x_{beam} = 200 \text{ \AA}$

5. Target

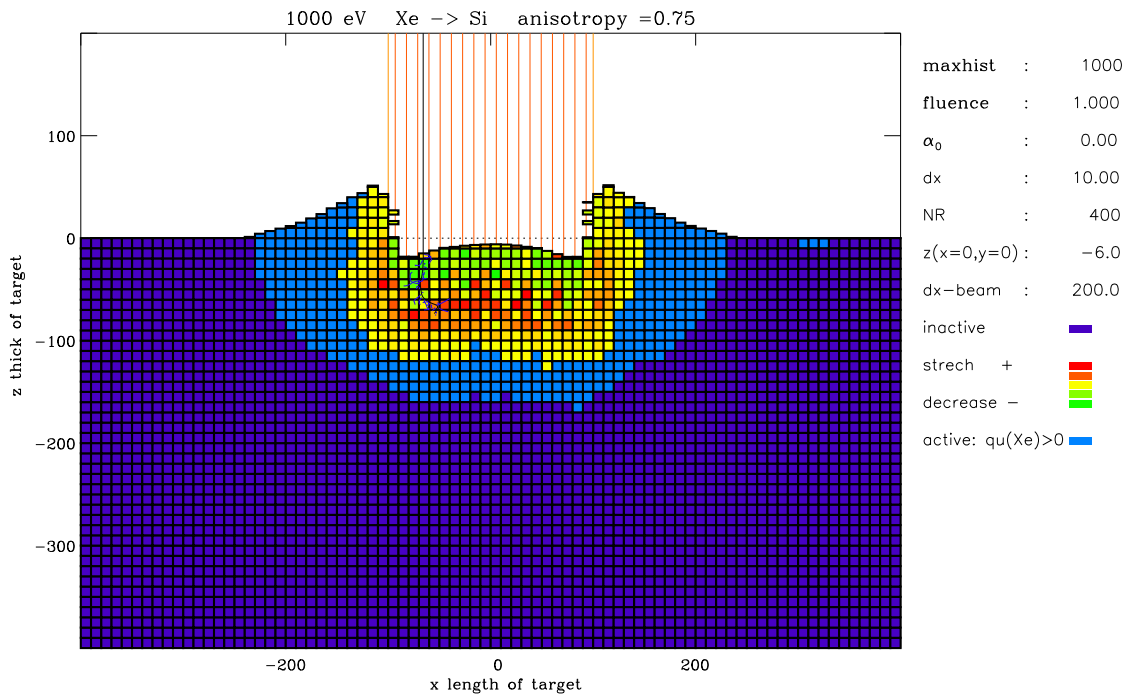


Figure 19: The target with vertical relaxation (anisotropy=0.75), $\Delta x_{beam} = 200 \text{ \AA}$

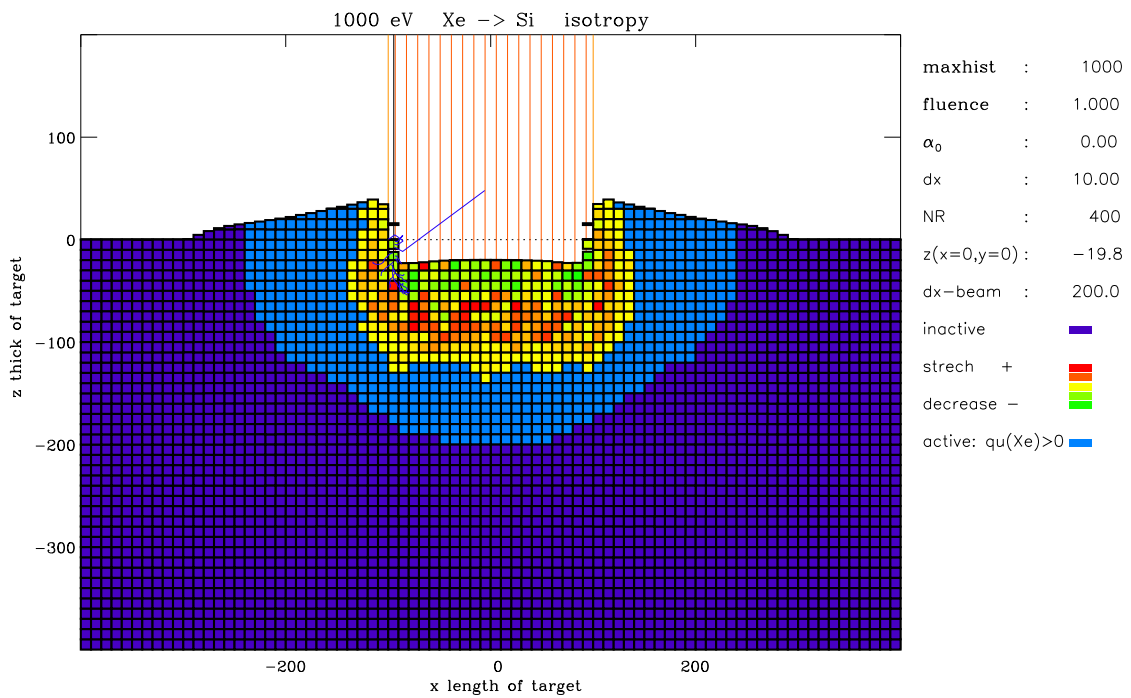


Figure 20: The target with isotropic relaxation, $\Delta x_{beam} = 200 \text{ \AA}$

5.8. Influence of the resolution

The influence of the resolution is shown in Fig. 21 - Fig. 23.

This is determined by the size of the cascade and where the important collisions take place. In this example a high resolution close to the surface is necessary, because there is a high gradient of composition.

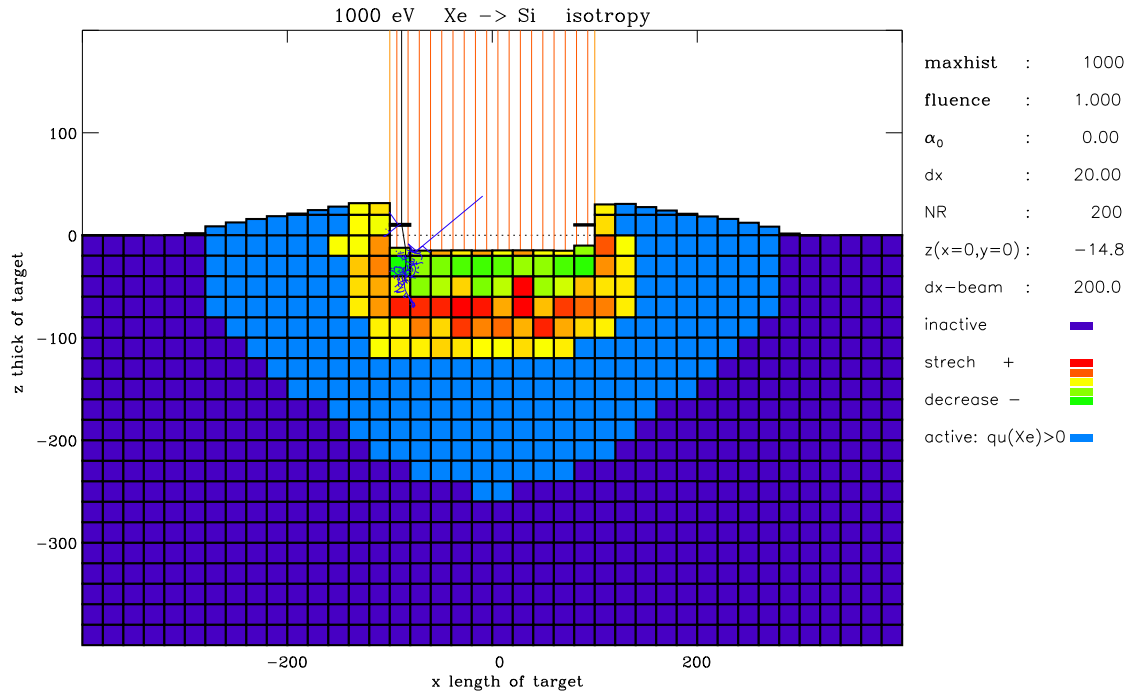


Figure 21: The target with cell resolution $\Delta x = 20 \text{ \AA}$, $\Delta x_{beam} = 200 \text{ \AA}$

5. Target

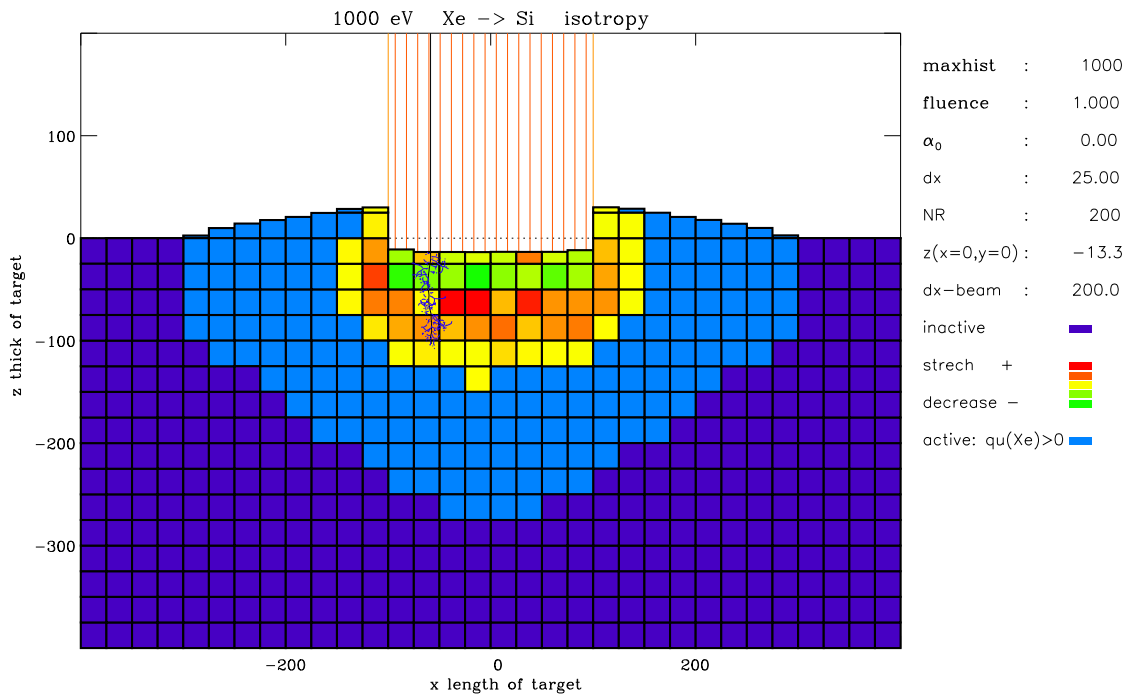


Figure 22: The target with cell resolution $\Delta x = 25 \text{ \AA}$, $\Delta x_{beam} = 200 \text{ \AA}$

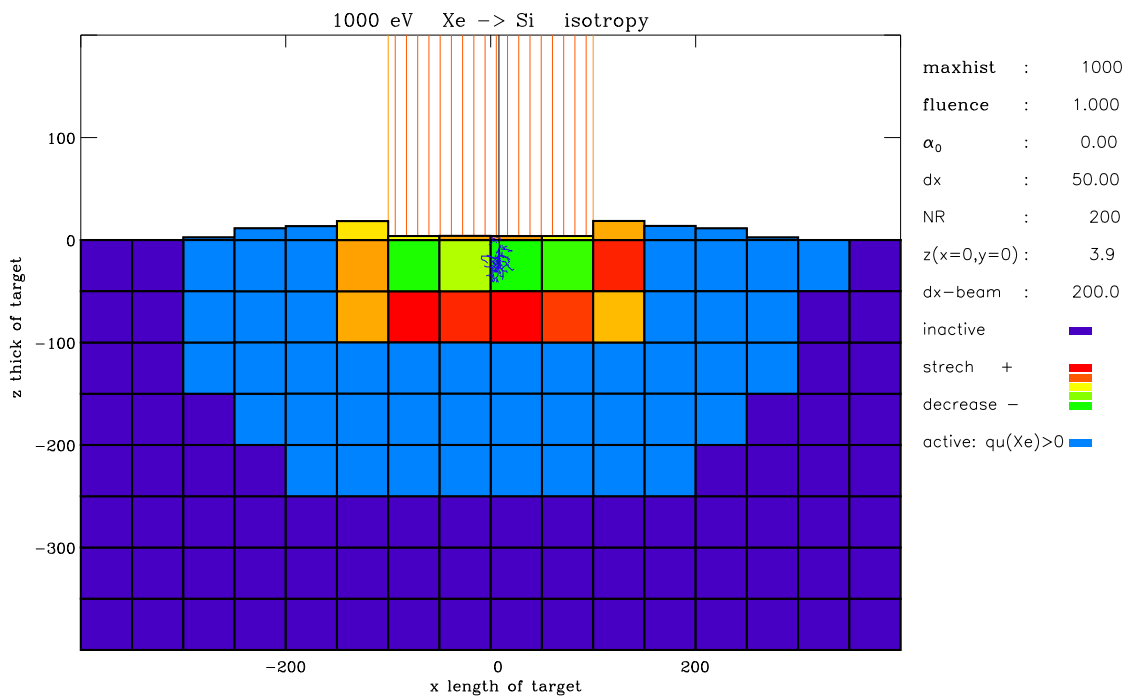


Figure 23: The target with cell resolution $\Delta x = 50 \text{ \AA}$, $\Delta x_{beam} = 200 \text{ \AA}$

6. Comparison of SDtrimSP and SDTrimSP-2D

In case of static calculations of the target, a two dimensional target and its resolution are irrelevant, unless there exists profiles in x and z directions.

In the dynamic case, but with 1-D targets, e.g. 1000 eV He on Ta_2O_5 , the difference between the results of 1-D and 2-D are small, Fig. 25 and Fig. 26.

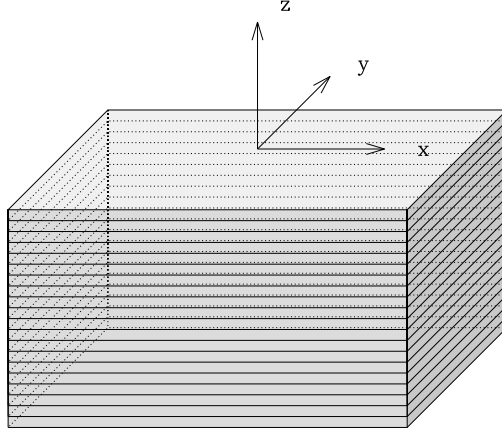


Figure 24: Geometry of one dimensional target, according to SDTrimSP

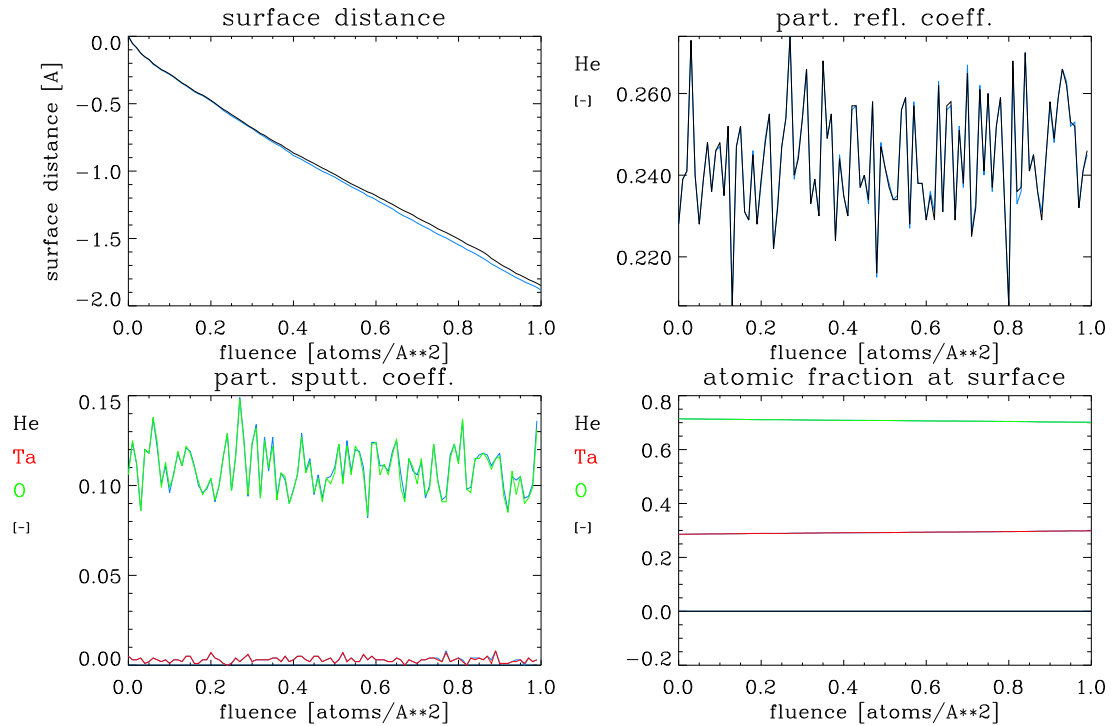


Figure 25: 1000 eV He on Ta_2O_5 , Comparison of results from SDTrimSP-2D and from SDTrimSP (blue)

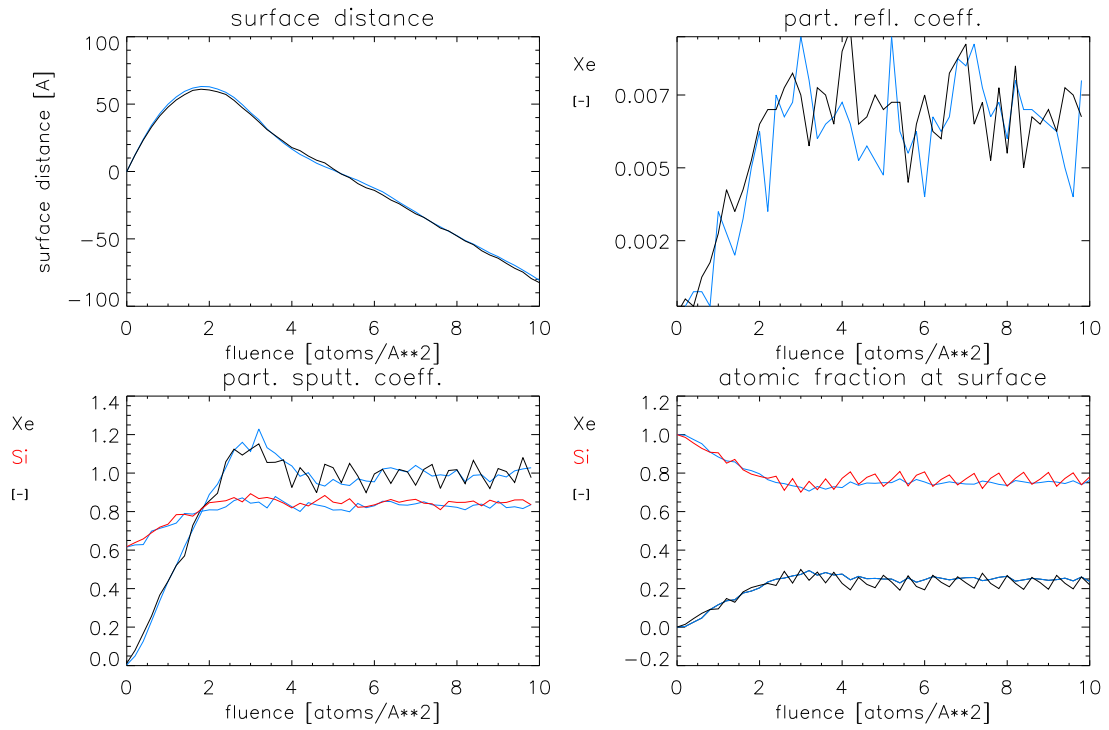


Figure 26: 1000 eV Xe on Si, Comparison of results from SDTrimSP-2D and from SDTrimSP (blue)

7. Two-Dimensional examples with SDTrimSP-2D

7.1. 1000 eV Xe on Si

This example is the bombarding of a silicon target with xenon. The thickness of cells is $\Delta z = 10 \text{ \AA} = 1 \text{ nm}$. The beam energy is 1000 eV , the fluence is $5.0 \frac{\text{atoms}}{\text{\AA}^2}$ and the cutoff-energy is 1.0 eV .

SDTrimSP gives a surface decrease of

$$D_0 = 25.4 \text{ \AA} \quad (7.71)$$

The 2-D-Model for a 1-D-simulation ($\Delta x, \Delta y \gg \Delta z$), see Fig. 24 and Fig. 27 gets for the surface decrease

$$D_1 = 24.1 \text{ \AA} \quad (7.72)$$

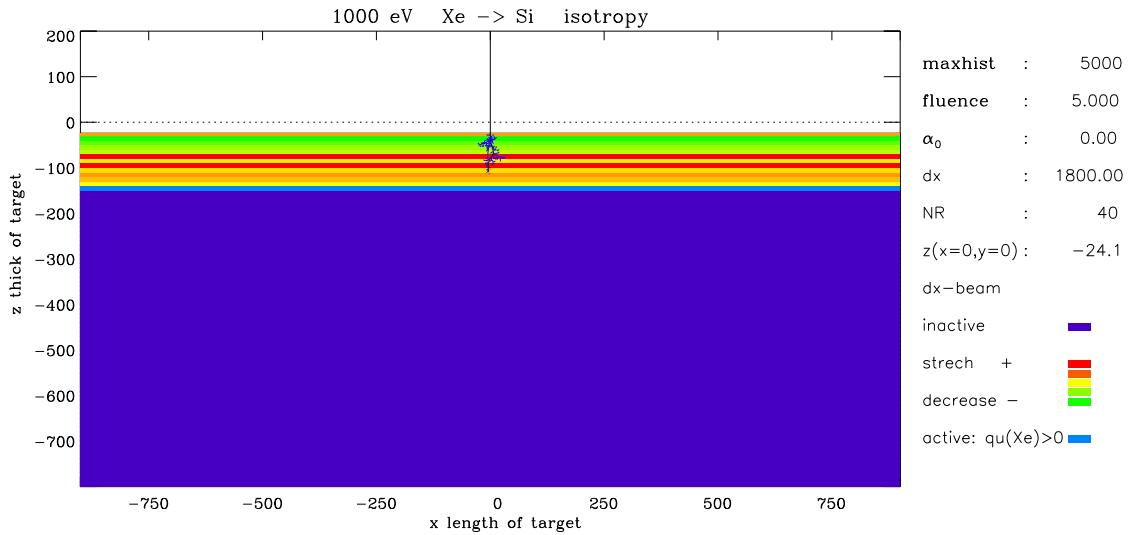


Figure 27: SDTrimSP-2D for 1-D-target

7. Two-Dimensional examples with SDTrimSP-2D

The target changes for 2-D cases ($\Delta y \gg \Delta x, \Delta z$) with different beam widths are shown in Fig. 28 - Fig. 33.

The surface decrease in the center of the beam $x = 0, y = 0$ are listed in Tab. 1. The penetration is dependent on the beam width. The simulation with a periodical beam produce the same results as the 1-D calculation.

nr.	Δx of beam	depth of indentation
1	50 \AA	148.3 \AA
2	100 \AA	129.5 \AA
3	200 \AA	89.4 \AA
4	400 \AA	57.9 \AA
5	800 \AA	35.4 \AA
5	periodical	24.6 \AA

Table 1: Surface decrease in the center of the beam

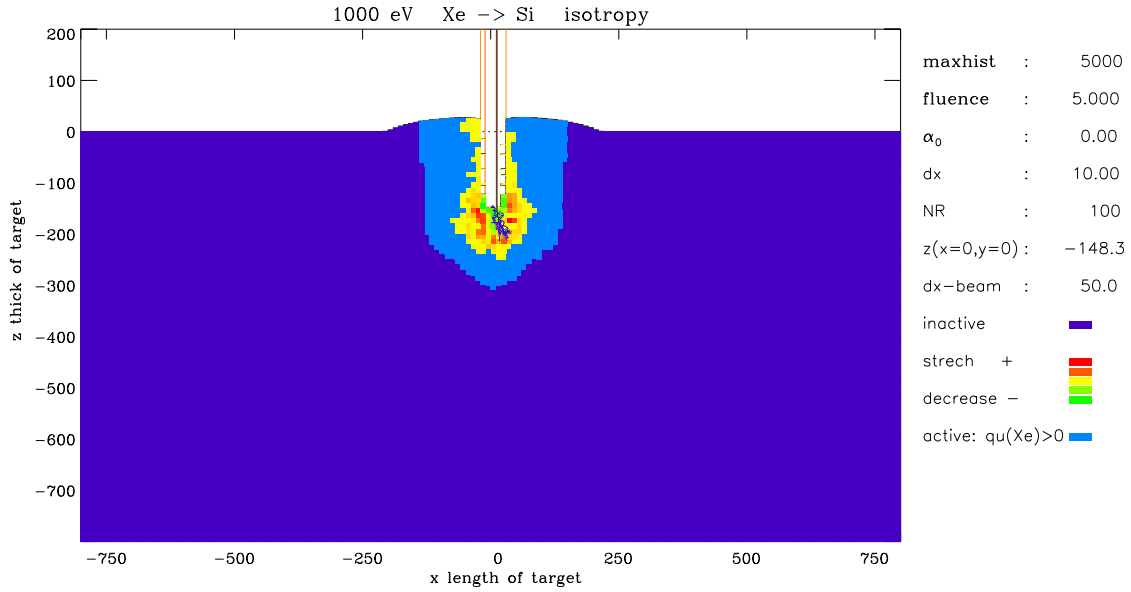
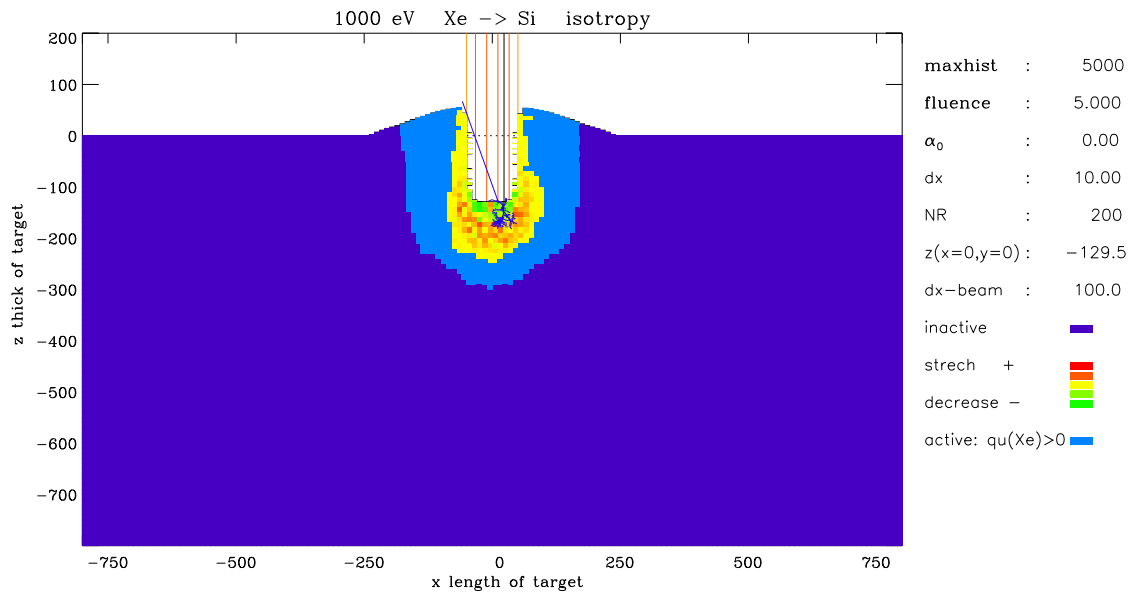
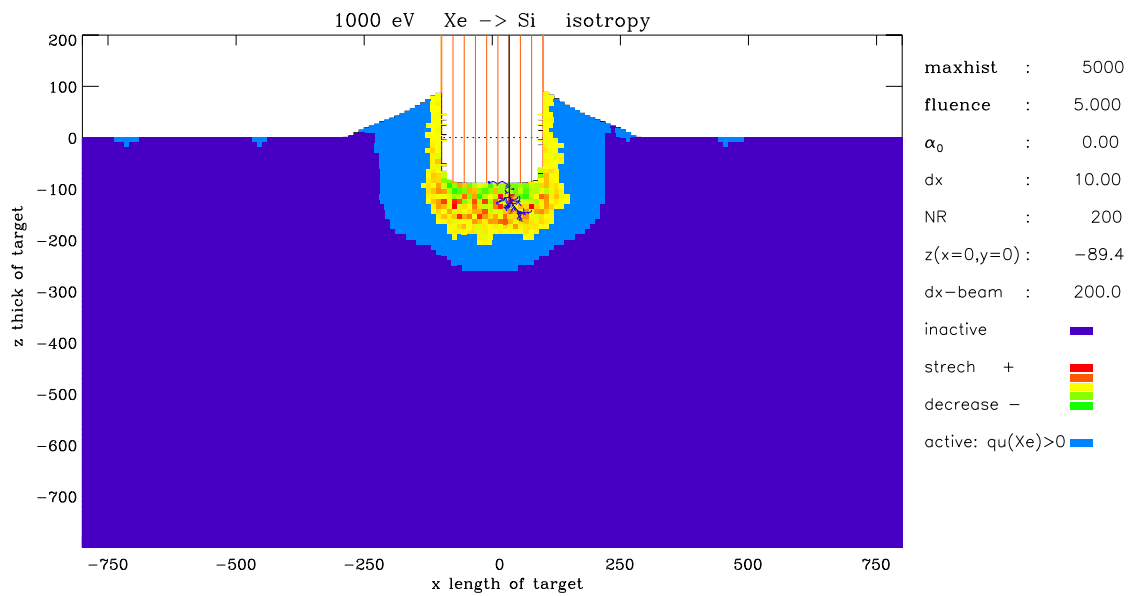


Figure 28: The target simulation $\Delta x_{beam} = 50 \text{\AA}$

Figure 29: The target simulation $\Delta x_{beam} = 100 \text{ \AA}$ Figure 30: The target simulation $\Delta x_{beam} = 200 \text{ \AA}$

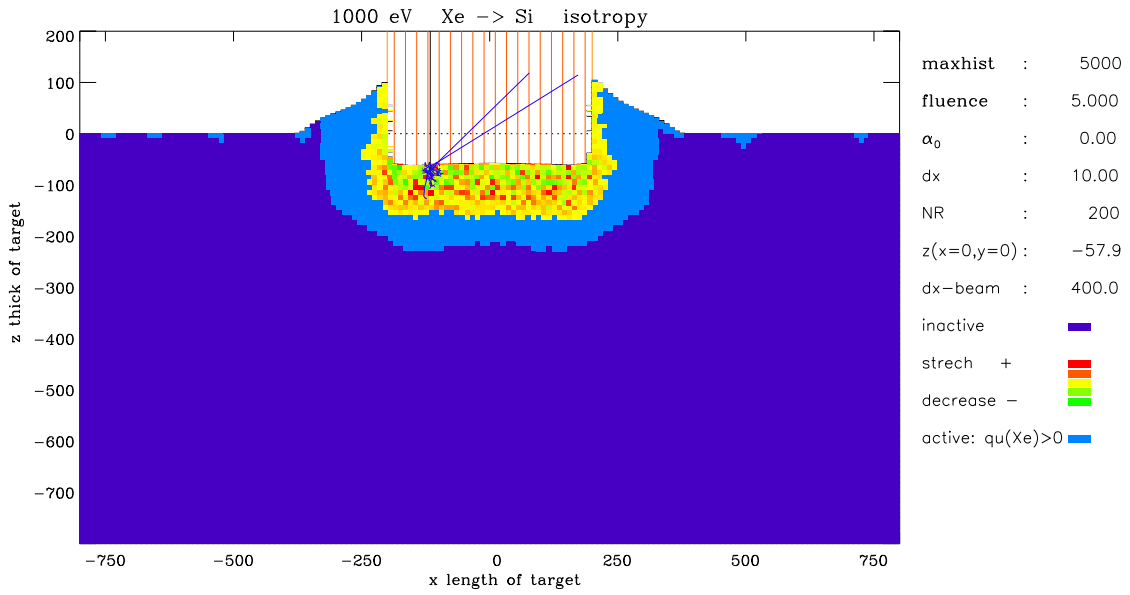


Figure 31: The target simulation $\Delta x_{beam} = 400 \text{ \AA}$

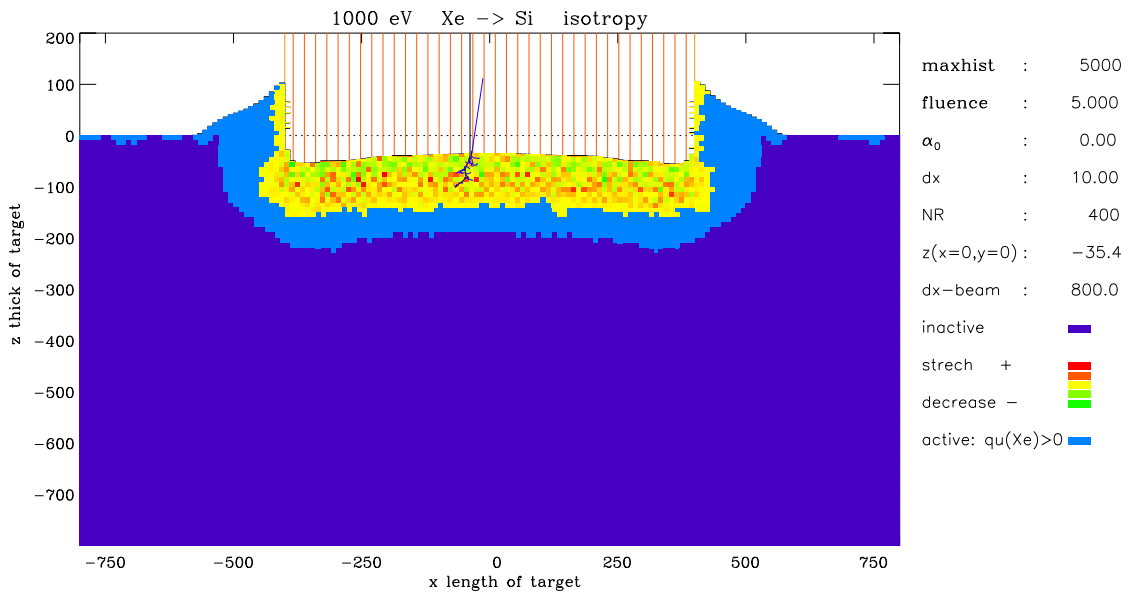


Figure 32: The target simulation $\Delta x_{beam} = 800 \text{ \AA}$

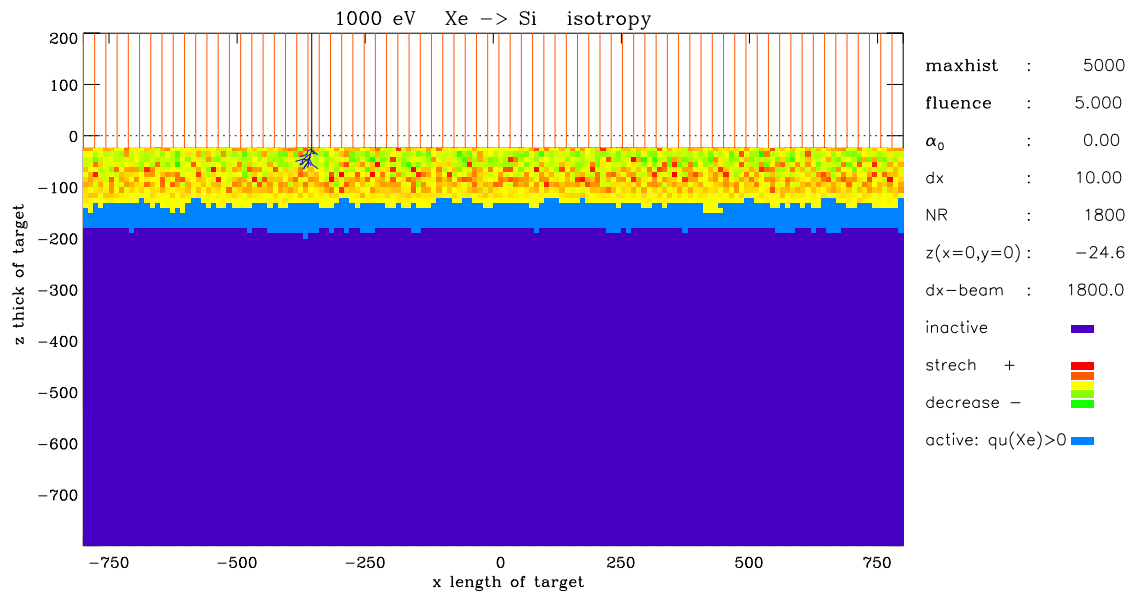


Figure 33: The target simulation with periodical beam and boundary conditions of target

7.2. 6 keV C on W

The next example is a bombardement of a W layer with C ions at normal incidence. The energy of incident ions is 6 keV.

The concentration of W and C in the target is changed due to the W sputtering and the implantation of C. The Fig. 34 shows the evolution of the elemental composition of a smooth and a rough target surface.

The calculated evolution of the surface profile with increasing fluence is shown in Fig. 35. The initial profile (fluence=0) is a measured profile from [8].

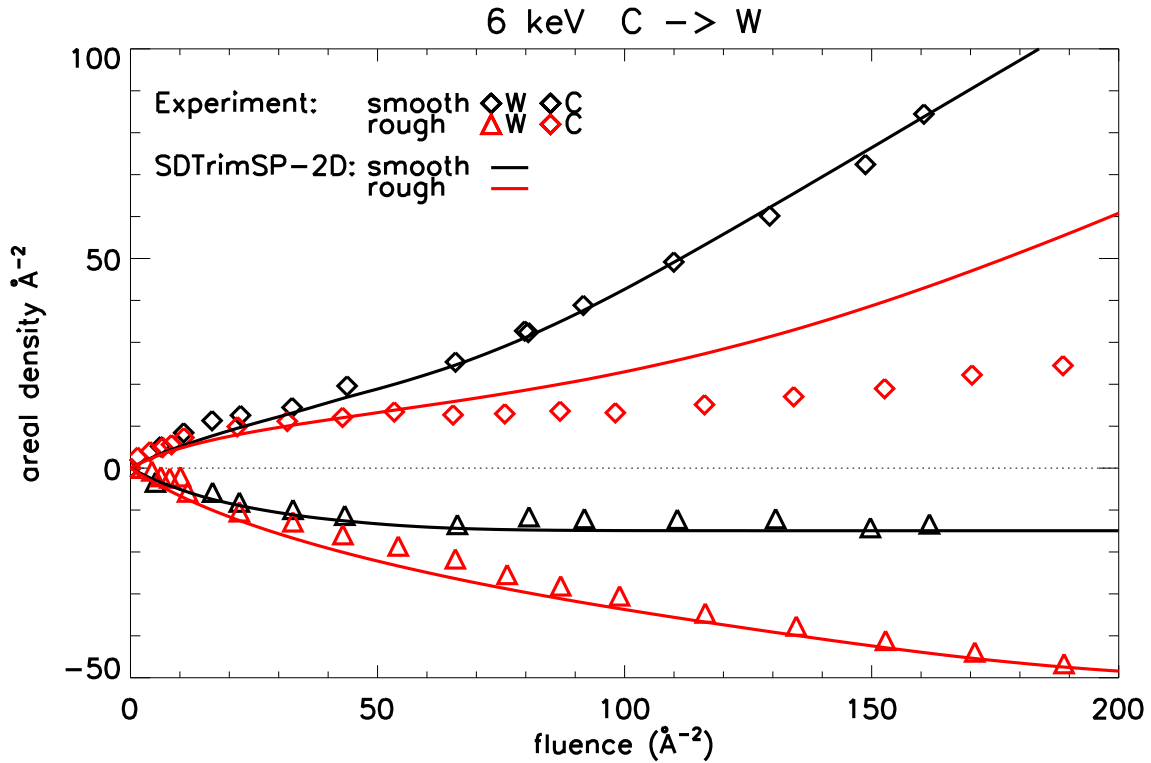


Figure 34: Calculated areal density of implanted C (positive values) and decrease W (negative values) versus the incident fluence compared with experimental data,[8]

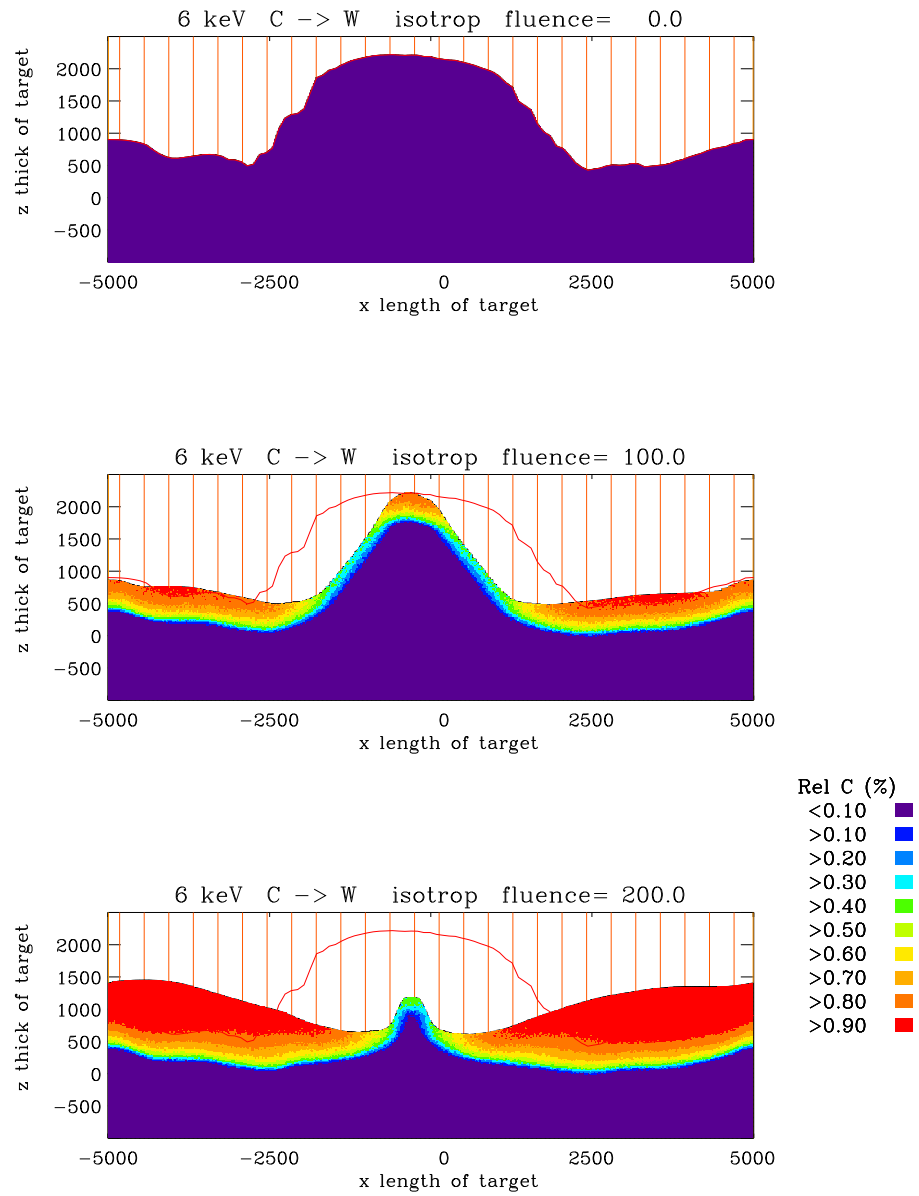


Figure 35: Numerical simulation of the evolution of the 2D profile as a result of the ion bombardement

References

- [1] D.Halliday,R.Resnick,J.Walker,*Fundamentals of Physics*, 2001, John Wiley & Sons, Inc.,New York
- [2] W. Eckstein, *Computer Simulation of Ion-Solid Interactions*, Springer Series in Material Science, Vol. 10, Springer Berlin, Heidelberg 1991
- [3] / W.Moeller,W.Eckstein, *TRIDYN-Binary Collision*, IPP 9/64, 1988
- [4] W.Moeller,W.Eckstein,*Tridyn-fzr-2001*, 2001
- [5] H.Schlager,W.Eckstein,*The scattering Integrals*, IPP 9/69, 1991
- [6] H.Friedrich,*Metall*, Fachbuchverlag Leipzig, 1983
- [7] S.Fronius,*Taschenbuch Maschininbau*, Verlag Technik Berlin, 1985
- [8] I.Bizyukov, K.Krieger, N.Azarenkov, U.v.Toussaint, J. Appl. Phys. 100(2006) 113302

A. Unit of physical terms

name	symbol	unit
mean free path	l_m	$\text{\AA} = 10^{-10}m$
random number	R_{random}	—
impact parameter	P_{impact}	$\text{\AA} = 10^{-10}m$
number of atoms	N	—
number of projectiles	NR	—
fluence	flc	$atom/\text{\AA}^2$
geometry of cell	$\Delta x, \Delta y, \Delta z$	\AA
pseudo time	τ	s
beam area	A_{flc}	\AA^2
volume	V	$\text{\AA}^3 = 10^{-30}m^3$
volumen-change	ΔV	\AA^3
atomic fraction	qu	—
length	L	$\text{\AA} = 10^{-10}m$
density	ρ	$g/\text{\AA}^3 = g/10^{-30}m^3$
atomic density	ρ_0	$atoms/\text{\AA}^3$
local coord. system	X_1, Y_2, Z_3	\AA
global coord. system	X_{3D}, Y_{3D}, Z_{3D}	\AA
polar angle	α_{pol}	$degree$
azimuthal angle	ϕ_{azi}	$degree$
energy of incident ion	e_{part}	eV
number of species	n_{cp}	—
surface of cell	$surf$	\AA^2

Table 2: Unit of physical terms